Songklanakarin J. Sci. Technol.
43 (5), 1351-1359, Sep. - Oct. 2021

http://www.sjst.psu.ac.th

Original Article

Isotherm, kinetics and thermodynamic studies of Cd^{2+} adsorption from aqueous solution onto cellulose nanocrystals obtained from cassava peel

C. V. Abiaziem[1, 2], C. T. Onwordi[3, 4], L. F. Petrik[3], and A. B. Williams[1*]

[1] *Department of Chemistry, Covenant University, Ota, Ogun, 112104 Nigeria*

[2] *Science Laboratory Technology Department, The Federal Polytechnic Ilaro, Ilaro, Ogun, 112106 Nigeria*

[3] *Department of Chemistry, Environmental and Nano Sciences Group, University of the Western Cape, Bellville, Cape Town, 7535, South Africa*

[4] *Department of Chemistry, Lagos State University, Ojo, Lagos, 102101 Nigeria*

Received: 1 July 2020; Revised: 7 October 2020; Accepted: 25 October 2020

Abstract

Cd^{2+} adsorption from aqueous solution onto cellulose nanocrystals from cassava peel (CP) was successfully studied. The sample was acid hydrolysed into cellulose nanocrystals using 64% sulphuric acid at 45°C for 45 min and was used as an adsorbent for the removal of Cd^{2+} from aqueous solution. Cellulose nanocrystals were characterised using high-resolution scanning electron microscope (HR-SEM), x-ray diffraction (XRD), and thermogravimetric analysis (TGA). The different optimization factors were studied. The adsorption equilibrium data were best fit by the Freundlich model with an R^2 of 1, indicating good surface heterogeneity of the active sites. Kinetic data were best fit by the pseudo-second order model type. The thermodynamic parameters enthalpy, entropy, and the negative change in Gibbs free energy, imply that the adsorption of Cd^{2+} onto CPCNC was exothermic, spontaneous, and feasible. This nanomaterial has good potential for use in successful removal of Cd^{2+} from wastewaters.

Keywords: adsorption, Cd^{2+}, cellulose nanocrystals, cassava peel, isotherm studies

1. Introduction

Water pollution caused by the indiscriminate dumping of untreated/partially treated industrial effluents laden with potentially toxic metals (PTMs) is one of the most serious environmental challenges facing the world today. These metals include lead, cadmium, arsenic, copper, and mercury among others, and are found in wastewaters, sourced from the weathering of sedimentary rocks, textile industry, printing or mining activities, etc.; they pose a serious threat to human beings and the environment at increasing concentrations (Anake, Benson, Akinsiku, Ehi-Eromosele, & Adeniyi, 2014). Amid these PTMs, cadmium ions are considered very toxic and poisonous to humans and the ecological environment (Satarug, 2012). At a high concentration the cadmium ions cause kidney dysfunction and renal failure; and at a low concentration, they lead to mutations by inducing oxidative deoxyribonucleic acid (DNA) damage and subsequent cancer (Methulakshmi & Anuradha, 2015).

In 2017, Nigeria produced 59 million tons of cassava, making it the world's largest producer at approximately 20% of global production, with a 37% increase in the last decade (IITA, 2020). Ogun State in Nigeria is one of the largest producers of cassava in Nigeria (Akerele, Idowu, Oyebanjo, Ologbon, & Oluwasanya, 2018), and the indiscriminate disposal of the peels of cassava changes the physicochemical and biological integrity of the environment.

*Corresponding author
Email address: akan.williams@covenantuniversity.edu.ng

This has necessitated finding uses for this cheap material, and it has potential for the removal of Cd^{2+} from aqueous solutions.

Chemically cassava peel (CP) is 40.5% cellulose (Widiarto, Pramono, Suharso, Rochliadi, & Arcana, 2019); or 37.9% cellulose, 23.9% hemicellulose, and 7.5% lignin (Tumwesigye, Morales-Oyervides, Oliveira, Sousa-Gallagher, 2016; while other studies have reported the cellulose content in CP as 93.24% (Widiarto, Yuwono, Rochliadi, & Arcana, 2017); or as 14.80% (Leite, Zanon, & Menegalli, 2017). This demonstrates that CP could be a good source of cellulose. Cellulose materials can be converted into nanocrystals that can serve as adsorbents for the uptake of PTMs from wastewater due to their unique properties, such as low density, reduced toxicity, high surface area, high tensile strength, biocompatibility, reactive hydroxyl groups that exhibit chemical functionalization, and biodegradability (Flauzino *et al*., 2016*)*.

However, in this study, the potential use of cellulose nanocrystals extracted from cassava peel was examined to remove Cd^{2+} from its aqueous solution. Therefore, the objectives of this research are (i) to characterize the prepared nanocrystals using high-resolution scanning electron microscopy (HR-SEM), X-ray diffraction (XRD), and thermogravimetric analysis (TGA), (ii) to investigate the effects of pH, initial concentration of Cd^{2+}, contact time, and temperature on Cd^{2+} adsorption efficiency, (iii) to analyze the equilibrium data using three candidate isotherm models (Freundlich, Langmuir, and Dubinin–Kaganer–Radushkevich (DKR)), (iv) to determine the kinetics and rate-controlling step in adsorption using three models (Pseudo-first and second-order models assessed by Sum of Squared Errors (SSE)), and (v) to determine the feasibility, spontaneity and randomness of the adsorption process from estimates of thermodynamic parameters (changes in standard Gibb's free energy(ΔG^o), Entropy(ΔS^o) and Enthalpy(ΔH^o)).

2. Materials and Methods

2.1 Materials and devices

The chemicals used were acetic acid, ethanol, sodium chlorite, sodium hydroxide, sulphuric acid, and toluene. All the reagents were of analytical grade and were purchased from Sigma Aldrich and Merck South Africa.

The devices used were centrifuge, sonicator **(**Misomix ultrasonic liquid processors**)**, pH meter **(**Mettler Toledo, SCS200-K**)**, freeze-dryer **(**Telstar LY Quest**:** HT 40**)**, orbital shaker **(**Ohaus centrifuge model FC5718**)**, heating mantle, X-ray diffraction spectroscope **(**Philips Xpert Pro-MPD x-ray diffractometer**)**, ICP-OES **(**Varian Radial, Varian 710-ES**)**, HR-SEM **(**AURIGA field emission high resolution scanning electron microscope, Zeiss, Germany**)**, and for thermogravimetric analysis a PerkinElmer Frontier TGA 4000 **(**Waltham, USA**)**.

2.2 Methods

2.2.1 Isolation of chemically purified cellulose

Raw cassava peels (RCP) used in this study were collected from different cassava processing plants at Ilaro and Owode areas in Ogun State, Nigeria. The sample was air-dried for several days, milled and sieved through a 30-mesh sieve. Chemically purified cellulose from cassava peel (CPCPC) was isolated according to the previously reported methods with slight modifications (Lu & Hsieh, 2012; Rahimi, Brown, Tsuzuki, & Rainey, 2016; Shaheen & Emam, 2018).

The cassava peel (30 g) was isolated with 2:1 v/v toluene and ethanol mixture for 6 h and then allowed to dry in an oven at 60°C for 16 h. The dewaxed sample was soaked in 50 g/L proportions in 5% sodium hydroxide solution at 25°C for 24 h, followed by heating at 90°C for 2 h to remove hemicellulose and silica. The solids were washed with a plentiful amount of distilled water until neutral pH was achieved, followed by drying at 50°C for 16 h. The residual alkaline treated sample was then delignified using 2.5% w/v of acidified sodium chlorite with fibre to liquor ratio of 1:20 for 4 h at 100°C. The delignified cellulose was, thereafter, washed with water to remove the excess/unreacted chemicals and dried in the oven at 50°C for 16 h. Finally, the product (chemically purified cellulose) was collected.

2.2.2 Extraction of cellulose nanocrystals

Chemically purified cellulose produced from the peel of cassava was converted into cellulose nanocrystals (CNC) by acid-hydrolysis, according to the methods adopted by Naduparambath *et al*. (2018) and Lu & Hsieh (2012), with slight modifications. The purified cellulose isolated from cassava peel was hydrolysed with 64 wt. % sulphuric acid at a 10 mL/g acid-to-cellulose ratio at a temperature of 45°C for 45 min with vigorous mechanical stirring. Hydrolysis reaction was quenched by diluting with 10-fold ice water. The resultant cellulose nanocrystal gel was centrifuged at 45,000 rpm for 30 min to concentrate the cellulose nanocrystals and to remove extra aqueous acid; the filtrate was then decanted. The resultant precipitate was dialyzed with a cellulose dialysis tube (Sigma –Aldrich, South Africa) against ultra-pure water until attaining neutral pH (pH 6-7). The suspension was sonicated at an amplitude of 40% in an ice bath to disrupt solid aggregates and avoid overheating. The resultant CNC suspension was freeze-dried (–47°C, 0.2 mbar). The dried sample was stored in an airtight container for characterization.

2.2.3 High-resolution scanning electron microscopy (HR-SEM)

HR-SEM (AURIGA Field Emission High-Resolution Scanning Electron Microscope, Zeiss, Germany), was used to analyze the superficial morphology of the raw and treated cellulose, and the nanocrystals. The samples were prepared by coating with carbon to make them conductive for SEM imaging. The HRSEM images were captured at varied magnifications.

2.2.4 X-ray diffraction (XRD) spectroscopy

X-ray diffraction was carried out using Philips X-pert MPD X-ray diffractometer with Cu-K radiation operating at 40 kV and 40 Ma, to identify the crystallinity in a material. The crystallinity index (C_I) was calculated from the maximum intensity of the principal peak of 200-plane (I_{002}, 2θ= 22.9°) and the intensity of diffraction of 110 peaks (I_{am}, 2θ=16°)

using the Seagal method (Azubuike, Rodríguez, Okhamafe & Rogers, 2012; Seagal, Creely, Martin & Conrad, 1959).

$$CI(\%) = \frac{I_{002} - I_{am}}{I_{002}} \times 100 \quad (1)$$

I_{002} represents crystalline material, whereas I_{am} represents amorphous material.

2.2.5 Thermal gravimetric analysis (TGA)

Thermal stability of RCP, CPCPC and CPCNC samples was determined using a Thermogravimetric Analyzer **(**PerkinElmer Frontier, TGA 4000, Waltham, USA**)**. An about 3.0 mg sample was weighed using a crucible sample holder and then placed in the machine. The TGA run was carried out under nitrogen atmosphere and the testing started at room temperature, ramped at 25ºC/min to 700ºC, and then held for 1 min at 700ºC.

2.2.6 Adsorption of cadmium ions

The adsorption of Cd^{2+} by cassava peel nanocrystals (CPCNC) was carried out in batch and in duplicate on a shaker at 200 rpm at 25ºC using 150 mL shaker flasks. The adsorption runs were designed to study the different operational factors using the synthesized cellulose nanocrystals. The pH was adjusted using 0.1M HCl or 0.1M NaOH to the maximum pH of 7 to avoid the formation of insoluble lead hydroxide. The Cd^{2+} in solution was analyzed using ICP-OES, and the adsorption capacity (q_e) and percentage removal were calculated as described in equations 2 and 3b, respectively.

$$q_e = \frac{(C_0 - C_e)V}{W} \quad (2)$$

$$R = \frac{C_0 - C_e}{C_0} \quad (3a)$$

$$R\% = \frac{C_0 - C_e}{C_0} \times 100 \quad (3b)$$

where, q_e is the equilibrium capacity of cadmium ions (mg/g), C_o is the amount of the cadmium ions in solution (mg/L), Ce is equilibrium amount of the cadmium ions in solution (mg/L), W is the dry weight of the nano-adsorbent (g), V = volume of the solution (L), and R% is the percentage of heavy metal removed/adsorbed.

2.2.7 Langmuir isotherm

Langmuir model assumes that every single adsorbed molecule meets the surface layer of the adsorbent (Ho, 2004). The linearized form of Langmuir model is:

$$\frac{1}{q_e} = \frac{1}{Q_m} + \frac{1}{Q_m b C_e} \quad (4)$$

q_e = Quantity of metal adsorbed per gramme of the adsorbent (mg/g)
Q_m = Maximum cover volume of the adsorbent (mg/g)
b = Langmuir isotherm constant (L mg^{-1})
C_e = Equilibrium concentration of the adsorbate (mg/L)

The values of q_e and b were evaluated from the slope and intercept of the Langmuir plot of $1/q_e$ against $1/C_e$. The Langmuir isotherm has as a constant (R_L), an equilibrium parameter.

$$R_e = \frac{1}{1 + (1+bC_0)} \quad (5)$$

Here C_0 = initial concentration of the adsorbate (mg/L)
b = Langmuir constant (L mg^{-1})

2.2.8 Freundlich isotherm

This model assumes a heterogeneous surface and is given by (Ahmad, Ahmad & Bello, 2014):

$$q_e = K_f C_e \frac{1}{N} \quad (6)$$

where,
q_e = amount of the heavy metal that had been adsorbed at equilibrium (mg/g)
K_f = Freundlich isotherm constant (mg/g)
n = adsorption intensity
C_e = equilibrium concentration of the adsorbate (mg/L)
1/N = the function of the strength of the adsorption
The linearized form of equation 6 for linear regression analysis is:

$$\ln q_e = \ln K_f + \frac{1}{N} \ln C_e \quad (7)$$

3. Results and Discussion

3.1 High-resolution scanning electron microscopy (HR-SEM)

Figure 1 shows the SEM images of cassava peel at different stages of processing. The smooth surface of the untreated sample (raw) in Figure 1a was due to the presence of some non-fibrous components on the fibers, such as lignin, hemicellulose, wax, pectin, oil etc. (Chen, Yu, Liu, Chen, Zhang, & Hai, 2011). After chemical treatment of the raw fibers, the surface of the CPCPC presented lump like structures seen in Figure 1b, which could be attributed to the strong intramolecular hydrogen bonds, while the smooth surfaces of the nanocrystals revealed that the treatment by sulphuric acid of cellulose fibers could have removed the intramolecular hydrogen bonds (Adewuyi and Vargas, 2016). Features of the cellulose nanocrystal in Figure 1c reveal that there was a decrease in the fibrillar structure size and intermittent breakdown in the fibrillar structure into individual fibrils. The SEM spectrum for CPCNC revealed a coarse, shattered, cracked surface, indicating high specific surface area with pores for the uptake of metal ions. The cracked surface allows free movement of the metal ions into the pores of the CPCNC; while the surface roughness contributes to a high specific surface area, facilitating strong adsorption of the

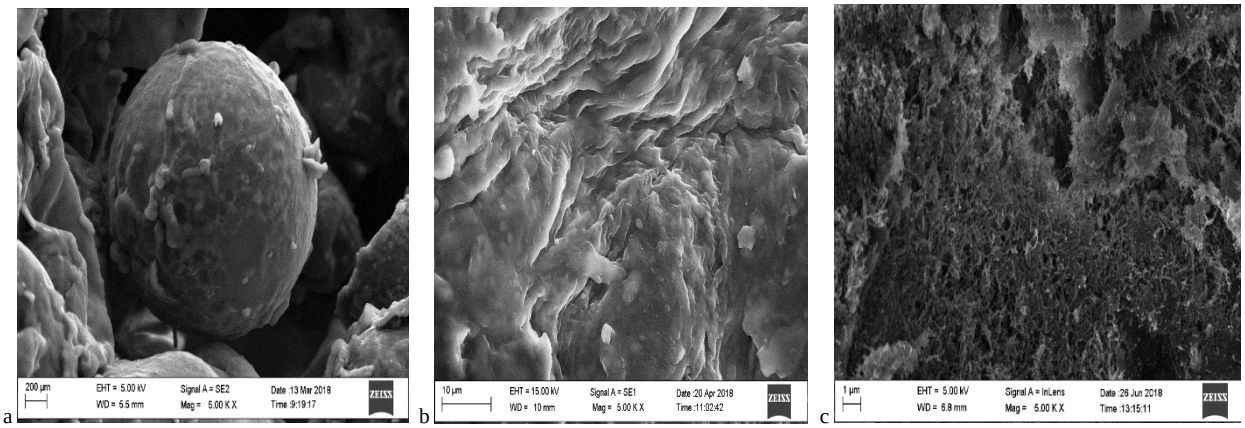

Figure 1. SEM micrographs of (a) raw cassava peel, processed to (b) cellulose, and (c) nanocrystals

metal ions by the pores of the adsorbent (Dada, Adekola & Odebunmi, 2015).

3.2 X-ray diffraction

The crystalline structure and phase purity of RCP, CPCPC and CPCNC were assessed from X-ray diffraction analysis, shown in Figure 2. The characteristic peaks for the raw sample were at 2θ= 17.65º, 15.02º and 34.19º which correspond to 110 and 400 lattice planes of cellulose, respectively, indicating the presence of lignin and hemicellulose (Lu & Hsieh, 2012). Also, the peak at 2θ= 12.39º and the disappearance of the peak for 400 lattice plane of cellulose indicate a partial removal of the amorphous regions (Thambiraj & Shankaran, 2017). The disappearance of the peak at 2θ=12.0º for CPCNC indicates complete removal of the amorphous domains. The three X-ray diffractograms showed the main peak at 2θ value of about 22.71°, indicating crystalline structure of cellulose in all samples (Flauzino *et al*., 2016). The crystallinity indexes of RCP, CPCPC and CPCNC were estimated to be 60.7%, 91.7%, and 99.9%, similar to the data obtained by Mohamed *et al*. (2017). The crystallinity index increased progressively from the raw to the CNC, showing a similar trend with results reported earlier (Rahimi *et al*., 2016). The progressive increase of crystallinity index from RCP to CNC indicates the removal of lignin, hemicellulose, and extractives (Widiarto, Yuwono, Rochliadi, Arcana, 2017). The XRD crystallite size estimates from RCP to CNC were 25.4 nm, 24.1 nm, and 5.56 nm.

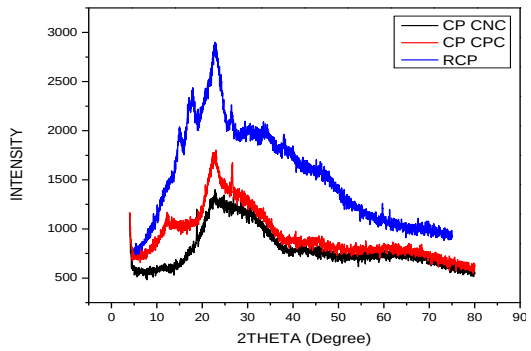

Figure 2. X-ray diffraction patterns of raw cassava peel (RCP), cellulose (CPCPC), and cellulose nanocrystals (CPCNC)

3.3 Thermogravimetric analysis (TGA)

Figures 3a and b present the TGA and differential thermal gravimetric (DTG) responses of RCP, CPCPC and CPCNC, and the raw cassava peel had three inflation points. The maximum degradation occurred at 75.3ºC due to the evaporation of moisture in the raw cassava peel. The CPCPC and CPCNC showed two inflation points. The disappearance of a peak was attributed to the chemical treatments that had removed non-cellulosic domains by breakdown of ether and carbon–carbon linkages (Joseph, Filho, James, Thomas & Carvalho, 1999). The peak within 300–400ºC which attained the optimum rate of disintegration was attributed to the glycosidic cleavage of cellulose. The CPCPC showed a weight loss at 100.5ºC due to moisture evaporation and a maximum degradation temperature at 349.5ºC. The thermogram of the nanocrystals showed a temperature of maximum degradation at 292.3ºC and onset temperature (reflecting thermal stability of the sample) at 218.2ºC: this was attributed to the attachment of sulphate groups on the surface of the nanocrystal cellulose during the sulphuric acid hydrolysis (Leãoa, Patrícia, João & Sandra, 2017). The results for the raw sample, the CPC and the CNC were similar to those reported by Hongjia, Yu, Longhui, & Xiong (2013). The TGA graphs indicate that the CNC was the least thermally stable because it degraded faster than the CPC and the RCP, and its uniform degradation was dissimilar to the raw case that had different thermal decomposition peaks.

3.4 Adsorption analysis of cadmium ions by CPCNC

effect of solution pH

Figure 4a presents the amount of Cd^{2+} adsorbed and the percentage Cd^{2+} removed by CPCNC at various choices of initial pH. It is observed that at a low pH the removal of Cd^{2+} increased and then decreased after pH 4, and reached an equilibrium at pH 7. The results show that the adsorption capacity of CPCNC adsorbent was dependent on the initial pH of the Cd^{2+} aqueous solution. This dependency decreases as soon as the pH tends towards neutrality: becoming steady due to the surface saturation of the adsorbent (Dada *et al*., 2015).

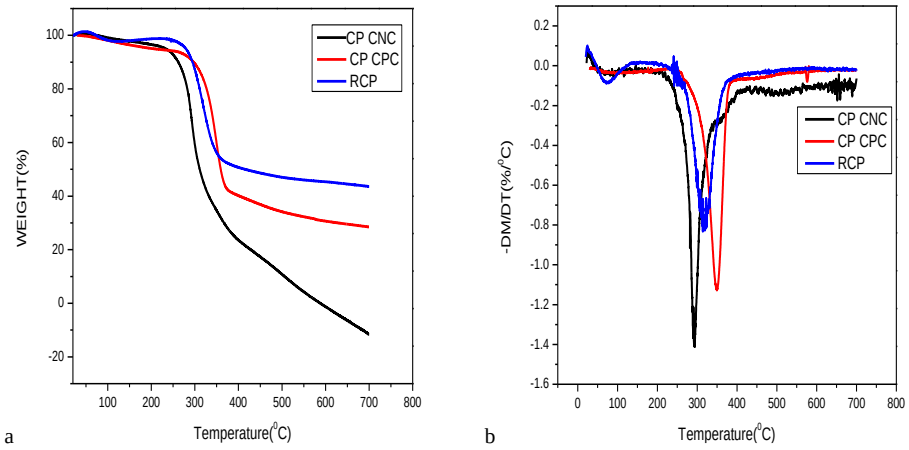

Figure 3. (a) TGA, and (b) DTG responses of raw cassava peel, cellulose, and nanocrystals

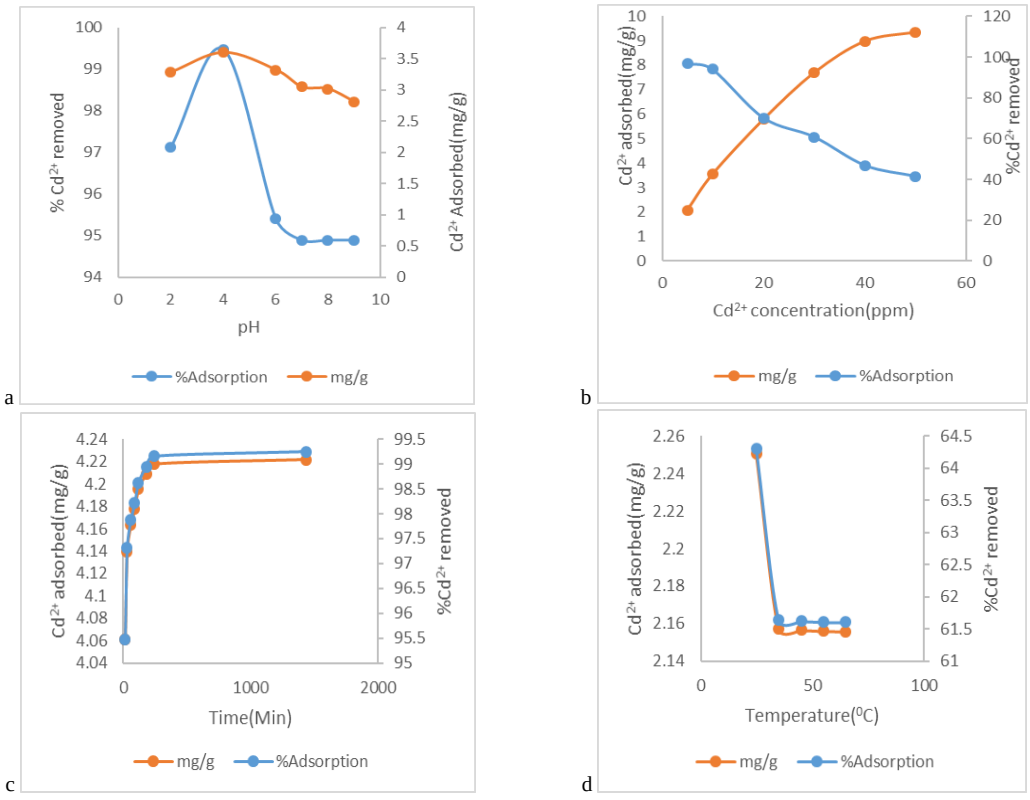

Figure 4. Effects of (a) pH, (b) initial Cd^{2+} concentration, (c) contact time, and (d) temperature on the adsorption of Cd^{2+} by CPCNC

The decrease in adsorption at high pH (pH≥6) is attributed to the formation of soluble hydroxyl complexes (Bode-Aluko, 2017). The adsorption characteristic was found to be dependent on pH, and the optimum adsorption was observed at pH 4 (99.5% and 3.60 mg/g).

3.5 Effect of initial Cd^{2+} concentration

Figure 4b presents the amount of Cd^{2+} adsorbed and the percentage removed by CPCNC at varying initial concentrations. The low percentage removal at higher metal ion concentrations was due to the fact that the adsorption sites became completely occupied and saturated; hence Cd^{2+} could not further be adsorbed from the solution. The maximum removal occurred at 5 ppm being 96.8%. From the results, cadmium adsorption was dependent on the initial metal ion concentration, and the findings are in agreement with an earlier report by Bode-Aluko, (2017). The increase in Cd^{2+} adsorption from 2.08 to 9.34 mg/g as the initial concentration was increased from 5 to 50 ppm was due to an increase in the mass transfer speed, attributed to the concentration gradient of Cd^{2+} in solution at the CPCNC nano-adsorbent surfaces.

3.6 Effect of contact time

Figure 4c represents the percentage of cadmium ion removal and the quantity of cadmium ions adsorbed. The results show that the amount of Cd^{2+} adsorbed increased from 4.06 to 4.22 mg/g with contact time change from 15 to 1440 min, and the percentage cadmium ion removal increased from 95.5 to 99.2% with this change. The stable increase in the adsorption rate from 15 to 240 min may be attributed to the accessibility of several sites for adsorption on the surfaces of the adsorbent, and the amount of Cd^{2+} adsorbed gradually reached a plateau from 240 to 1440 min where there was no significant further removal of metal ions, due to the fact that CPCNC active sites had been saturated with cadmium metal ions. This result is similar to that earlier reported (Dada *et al*., 2015).

3.7 Effect of temperature

Figure 4d represents the percentage removal, and the amount of Cd^{2+} adsorbed against temperature. The percentage of adsorption removal decreased from 64.3 to 61.6% with temperature increase from 25 to 45ºC; and the removal reached a steady level at 55ºC. The amount of cadmium ions adsorbed decreased very rapidly from 2.25 to 2.15 mg/g with the temperature change from 25 to 35ºC. However, in 35-65ºC there was no significant change, indicating that the adsorption capacity had reached a steady level; this further indicates that the active adsorbent sites were saturated with metal ions at the higher temperatures (Dada *et al*., 2015). The optimum percentage removal and amount of Cd^{2+} adsorbed (64.3% and 2.25 mg/g) occurred at 25ºC.

3.8 Adsorption isotherms

3.8.1 Langmuir, Freundlich and DKR isotherms for adsorption of Cd^{2+} onto CPCNC

Figures 5a and 5c show the Langmuir and Freundlich plots for adsorption of Cd^{2+} onto CPCNC. The parameter estimates and coefficients of determination (R^2) are summarized in Table 1. Based on the latter, the experimental data were best fit by the Freundlich model with R^2 value of 1, while the Langmuir model had an R^2 value of 0.9984. These suggest a good surface heterogeneity of the active sites and the formation of a monolayer of adsorbate on surfaces of the CPCNC, respectively (Dada, Ojediran & Abiodun, 2013). The Freundlich plot for adsorption of Cd^{2+} onto CPCNC showed that the constants n and K_f were derived from the plot of Lnq_e against LnC_e. The value of n is 1, which is far less than 10, indicating that the adsorption was favorable; and 1/n indicates the strength of the adsorption and its heterogeneity which in the range from 0 to 1 suggests a good adsorption intensity (Bode-Aluko, 2017; Dada *et al*., 2015).

The Langmuir parameter b was 0.0083 mg/L, which indicates the adsorption bond between adsorbent and Cd^{2+}. Strong bond energy between the adsorbent and the metal ion leads to a high adsorption capacity (Dada *et al*., 2015; Yu *et al*., 2013). The equilibrium parameter, R_L, is an important integral of the Langmuir isotherm, as shown in Figure 5b, and is the separation factor, a dimensionless constant (Dada *et al*., 2015). The R_L value indicates whether the adsorption is favorable or unfavorable. If $R_L>1$ it is unfavorable, if $R_L= 0$ it is irreversible, if $R_L=1$ it is linear, and if $0<R_L<1$ it is favorable and feasible. In the adsorption of Cd^{2+} onto CPCNC,

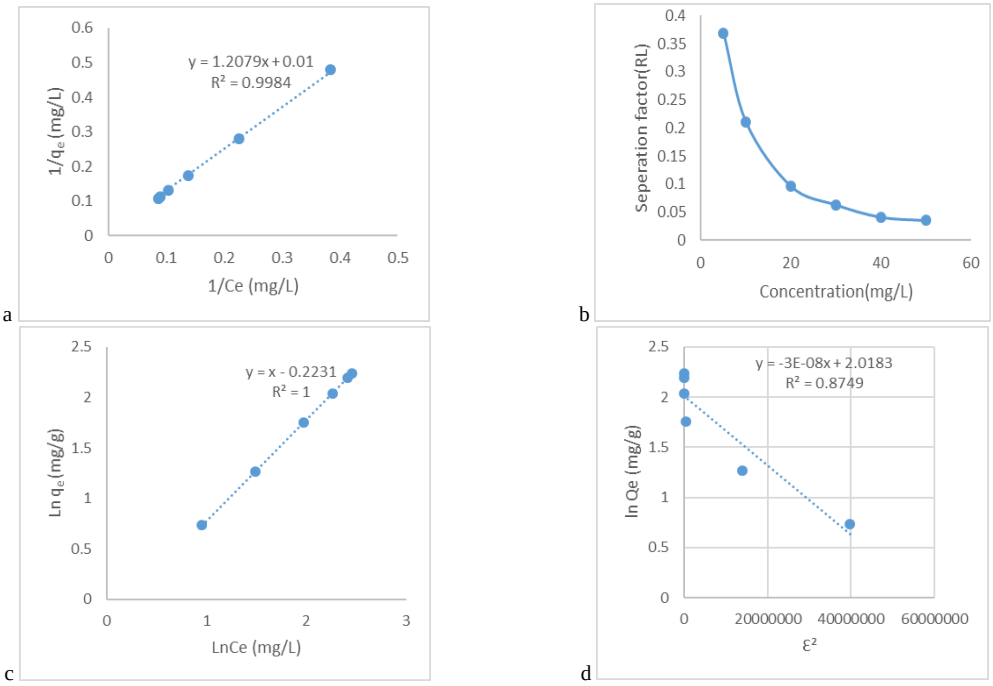

Figure 5. (a) Langmuir isotherm, (b) R_L value for the adsorption of Cd^{2+} by CPCNC, (c) Freundlich isotherm, and (d) DKR isotherm fits for the adsorption of Cd^{2+} by CPCNC

Table 1. Estimates of parameters in isotherm models for the adsorption of Cd^{2+} by CPCNC

Freundlich	Langmuir	DKR
n = 1	Qm = 100	Q_d = 7.526
1/n = 1	b = 0.0083	A_{DRK} = -3x10^{-8}
K_f = 1.250	R_L = 0.035-0.369	E(KJ/mol) = 4.08
R^2 = 1.000	R^2 = 0.9984	R^2 = 0.8749

the values of R_L ranged from 0.035 to 0.369, staying below 1, and indicating that the adsorption was favorable and feasible. Based on the R^2 value of the DKR model, which was 0.8749, the adsorption data were less well fit by the DKR model as presented in Figure 5d and Table 1. Since the magnitude of E, the free energy of transfer of solute ions to the surface of the adsorbent material, CPCNC, was below 8 KJ/mol, the adsorption mechanism was physisorption, and the mean adsorption energy E, calculated from DKR isotherm was 4.08 KJ/mol, which reveals that the electrostatic forces played an important role in the adsorption process. These findings are supported by earlier reports (Dada *et al*., 2015; Dada, Adekola & Odebunmi, 2017).

3.8.2 Adsorption kinetics

In determining the adsorption rate-controlling step of Cd^{2+} onto the nano-adsorbent, pseudo-first order and pseudo-second order models were used as candidate models of the heavy metal adsorption kinetics. The conformity of the experimental values with the models were assessed from the coefficient of determination. Figures 6a and 6b represent the pseudo-first and pseudo-second order adsorption kinetics plots, respectively. The evaluated parameters of the pseudo-first and pseudo- second order models are presented in Table 2. Based on the R^2 values, the adsorption kinetics data were best fit by the pseudo-second order kinetics with an R^2 value of 1, greater than 0.99, while R^2 for the pseudo-first order model was 0.7024. In Table 2, the rate of reaction for pseudo-second order was clearly higher than that for the pseudo-first order model. The calculated amount of Cd^{2+} adsorbed onto CPCNC was $q_{e\ cal}$ (4.228) which was closer to the experimental amount of Cd^{2+} adsorbed $q_{e\ exp}$ (4.178) from the pseudo-second order model, signifying that the kinetics of Cd^{2+} adsorption were best fit by the pseudo-second order model, implying that the adsorption process had chemisorption as the rate-determining step (Dada *et al*., 2015). The applicability of pseudo-first order and pseudo-second order models was judged from R^2 and the sum of squared errors (SSE). The closer the R^2 is to unity, the lower the SSE, and the better the model describes the adsorption of Cd^{2+} onto CPCNC. Based on this, the pseudo-second order model gave the better fit while a poorer description was obtained with the pseudo-first order model.

3.8.3 Adsorption thermodynamics

Thermodynamics are significant for adsorption studies because of the vital parameters to be determined. Figure 7 presents the Van't Hoff plot for the adsorption of Cd^{2+} by CPCNC. A summary of the evaluated parameters is presented in Table 3. The enthalpy change and the entropy

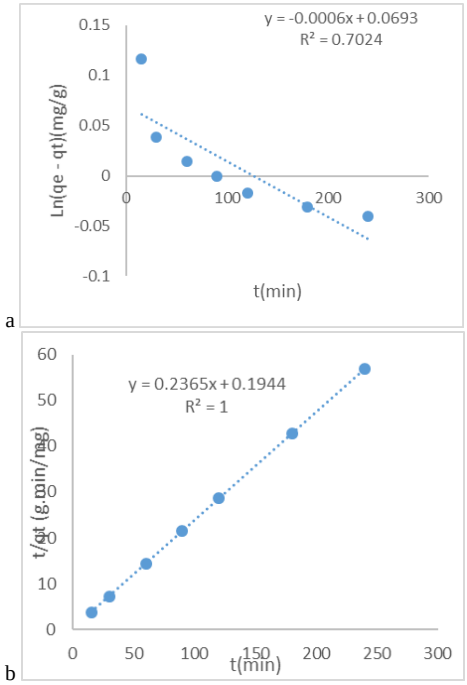

Figure 6. (a) and (b): Pseudo-first order and pseudo-second order kinetics plots for the adsorption of Cd^{2+} by CPCNC

Table 2. Kinetic model parameter estimates for the adsorption of Cd^{2+} by CPCNC

Pseudo-first order model	Pseudo-second order model
q_{eexp} = 4.178	q_{eexp} = 4.178
q_{ecal} = 1.072	q_{ecal} = 4.228
K_1 = 0.0445	K_2 = 0.288
h_1 = 0.051	h_2 = 5.149
SSE = 1.174	SSE = 0.019

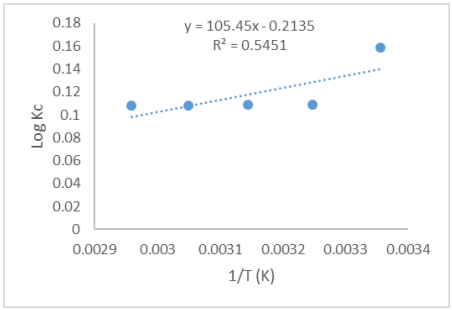

Figure 7. Van't Hoff plot for the adsorption of Cd^{2+} by CPCNC

change were determined from the slope and intercept of the Van't Hoff plot, respectively. The negative enthalpy change implies that the adsorption of Cd^{2+} onto CPCNC is exothermic in nature. The negative entropy change confirmed the degree of uncertainty at the solid-liquid relationship in the course of the adsorption of Cd^{2+} onto CPCNC. The negative Gibbs free energy indicates that the adsorption process was spontaneous and feasible. These findings are in agreement with reports from other studies (Dada *et al*., 2015; Garima, 2013).

Table 3. Thermodynamic parameters for the adsorption of Cd^{2+} by CPCNC

T (°C)	T(K)	ΔG(KJmol^{-1})	ΔH(KJ^{-1})	ΔS(Jmol^{-1}K^{-1})
25	298	-800.842	-2019.066	-4.088
35	308	-759.962		
45	318	-719.082		
55	328	-678.202		
65	338	-637.322		

4. Conclusions

In this study, cellulose nanocrystals from cassava peel have shown good prospects for use as nano-adsorbent material in the purification of Cd^{2+} polluted water. The results indicate that the adsorption of Cd^{2+} hinged on all the tested factors, namely pH, initial concentration of Cd^{2+}, contact time, and temperature. The adsorption equilibrium data were best fit by the Freundlich model with an R^2 of 1, while the Langmuir model had an R^2 of 0.9984, indicating a good surface heterogeneity of the active sites. The mean adsorption energy E, estimated from DKR isotherm, was 4.08 KJ/mol, which revealed that the electrostatic forces played an important role in the adsorption process. The kinetics of adsorption were well described by a pseudo-second order kinetic model, and the process of adsorption may be chemical adsorption. The thermodynamics revealed that the adsorption process was exothermic, feasible, and spontaneous in nature. Overall this study revealed a good adsorption of Cd^{2+} by the CPCNC adsorbent. Hence, cellulose nanocrystals from cassava peel are a candidate low-cost alternative nano-adsorbent material for the removal of Cd^{2+} from polluted waters.

Acknowledgements

The authors sincerely appreciate the financial contributions of TETFUND (Nigeria) through Federal Polytechnic Ilaro, under grant number [AD/R/SC/57/ VOL.12/819], NRF/RISA (South Africa), grant number [KIC180412320000], Mr. Yunus Kippie of School of Pharmacy, University of the Western Cape, Cape Town, South Africa and the support of Professor Leslie Petrik for offering the laboratory space and equipment of Environmental and Nano Science Group, University of the Western Cape. Thanks to Ilse Wells for assisting in the cadmium solution analysis.

References

Adewuyi, A., & Vargas, P. F. (2017). Chemical modification of cellulose isolated from underutilised hibiscus sabdariffa via surface grafting: A potential bio-based resource for industrial application. *Chemistry in Industry, 66(7-8),* 327-338.

Ahmad, M. A., Ahmad, N., & Bello, O. S. (2014). Modified durian seed as adsorbent for the removal of methyl red dye from aqueous solutions. *Applied Water Science, 5(1),* 407-423. doi:10.1007/s13201-014-0208-4

Akerele, E. O., Idowu, A. O, Oyebanjo, O., Ologbon, O. A. C. & Oluwasanya, O. P. (2018). Economic analysis of cassava production in Ogun State, Nigeria. *Acta Scientific Agriculture, 2(8),* 43-50.

Anake, W. U., Benson, N. U., Akinsiku, A.A., Ehi Eromosele, C. O., & Adeniyi, I. O. (2014). *Assessment of trace metals in drinking water and groundwater sources in Ota, Nigeria. International Journal of Scientific and Research Publications, 4 (5),* 1-4.

Azubuike, C. P., Rodríguez, H., Okhamafe, A. O., & Rogers, R. D. (2012). Physicochemical properties of maise cob cellulose powders reconstituted from ionic liquid solution. *Cellulose, 19(2),* 425–433.

Bode-Aluko, C. A. (2017). *Functionalisation of polymer nanofibres and track-etched membrane for removal of organic and inorganic pollutants from water* (Doctoral thesis, University of the Western Cape, Cape Town, South Africa).

Chen, W. S., Yu, H. P., Liu, Y. X., Chen, P., Zhang, M. X., & Hai, Y. F. (2011). Individualisation of cellulose nanofibers from wood using high-intensity ultrasonication combined with chemical pretreatments. *Carbohydrate Polymer, 83(4),* 1804–1811. doi:10.1088/2043-6262/7/3/035004.

Dada A. O, Adekola, F. A., & Odebunmi, E. O. (2017). Kinetics, mechanism, isotherm and thermodynamic studies of liquid-phase adsorption of Pb^{2+} onto wood activated carbon-supported zerovalent iron (WAC-ZVI) nanocomposite. *Cogent Chemistry, 3,* 1351653. doi:10.1080/23312009.2017.1351653.

Dada, A. O., Adekola, F. A., & Odebunmi, E. O. (2015). A novel zerovalent manganese for removal of copper ions: synthesis, characterisation and adsorption studies. *Applied Water Science.* doi:10.1007/ s13201-015-0360-5.

Dada, A. O., Ojediran, J. O., & Abiodun, P. O. (2013). Sorption of Pb^{2+} from aqueous unto modified rice husk: Isotherm studies. *Advances in Physical Chemistry, 2013,* 1-6. Article ID 842425. doi:10. 1155/2013/842425.

Flauzino, N. W. P., Mariano, M., da Silva, I. S. V., Putaux, J. L., Otaguro, H., Pasquini, D., & Dufresne, A. (2016). Mechanical properties of natural rubber nanocomposites reinforced with high aspect ratio cellulose nanocrystals isolated from soy hulls. *Carbohydrate Polymers, 153,* 143-152.

Garima, J. (2013). *Removal of copper and zinc from wastewater using chitosan (*Master's dissertation, National Institute of Technology, Rourkela Orissa, India).

Ho, Y. S. (2004). Pseudo-isotherms using a second order kinetic expression constant. *Adsorption, 10,* 151–158.

Hongjia, L., Yu, G., Longhui, Z & Xiong, L. (2013). Morphological, crystalline, thermal and physicochemical properties of cellulose nanocrystals obtained from sweet potato residue. *Journal of Food Research International, 50,* 121–128.

International Institute of Tropical Agriculture. (2020, September 26). Cassava. Retrieved from https:// www.iita.org/cropsnew/cassava/.

Joseph, K., Filho, R. D. T., James, B., Thomas, S. & Carvalho, L. H. (1999). A review on sisal fiber reinforced polymer composites. *Revista Brasileira de Engenharia Agricola e Ambiental, 3*, 379.

Leãoa, R. M., Patrícia, C. M., João, M. L. L. M. & Sandra, M. L. (2017). Environmental and technical feasibility of cellulose nanocrystal manufacturing from sugarcane bagasse. *Carbohydrate Polymers, 175*, 518–529.

Leite, A. L. M. P., Zanon, C. D. & Menegalli, F. C. (2017). Isolation and characterization of cellulose nanofibers from cassava root bagasse and peelings. *Carbohydrate Polymers, 157*, 962–970.

Lu, P., & Hsieh, Y. (2012). Preparation and characterisation of cellulose nanocrystals from rice straw. *Carbohydrate Polymers, 87*, 564– 573.

Methulakshmi, A. N., & Anuradha, J. (2015). Removal of cadmium ions from water/wastewater using chitosan**.** Research & Reviews**.** *Journal of Ecology and Environmental Sciences, 1*, 9-14**.**

Mohammad, M. A., Salleh, W. N. W., Jaafar, J., Ismail, A. F., Mutalib, M. A., Mohamada, A. B., . . . Mohd Hir, Z. A. (2017). Physicochemical characterisation of cellulose nanocrystal and nanoporous self-assembled CNC membrane derived from Ceibapentandra. *Carbohydrate Polymers, 157*, 1892–1902.

Naduparambath, S., Jinitha, T. V., Shaniba, V., Sreejith, M. P., Aparna, K. B., &Purushothaman, E. (2018). Isolation and characterisation of cellulose nanocrystals from sago seed shells. *Carbohydrate Polymers, 180*, 13–20.

Rahimi, M. K. S., Brown, R. J., Tsuzuki, T., & Rainey, T. J. (2016). A comparison of cellulose nanocrystals and cellulose nanofibres extracted from bagasse using acid and ball milling methods. *Advances in Natural Sciences: Nanoscience and Nanotechnology, 7*, 1-9. doi:10.1088/2043-6262/7/3/035004

Satarug, S. (2012). Long-term exposure to cadmium in food and cigarette smoke, liver effects and hepatocellular carcinoma. *Current Drug Metabolism, 13(3),* 257-271.

Seagal, L., Creely, J. J., Martin, A. E., & Conrad, C. M. (1959). An empirical method for estimating the degree of crystallinity of native cellulose using X-ray diffractometer. *Textile Research Journal, 29*, 786–794.

Shaheen, T. I., & Emam, H. E. (2018). Sono-chemical synthesis of cellulose nanocrystals from wood sawdust using acid hydrolysis. *International Journal of Biological Macromolecules, 107*, 1599–1606.

Thambiraj, S., & Ravi, S. D. (2017). Preparation and physicochemical characterisation of cellulose nanocrystals from industrial waste cotton. *Journal of Applied Surface Science, 412*, 405–416.

Tumwesigye, K. S., Morales-Oyervides, L., Oliveira, J. C., Sousa-Gallagher, M. J. (2016). Effective utilisation of cassava bio-wastes through integrated process design: A sustainable approach to indirect waste management. *Process Safe Environmental Protection, 102*, 159–167

Widiarto, S**.**, Yuwono, S**.** D**.**, Rochliadi, A**.** & Arcana, I**.** M**.** **(**2017**).** Preparation and characterisation of cellulose and nanocellulose from agro-industrial waste - cassava peel. *IOP Conference Series: Material Science and Engineering, 176*, 1-6. 012052 doi:10.1088/1757-899X/176/1/012052.

Widiarto, S., Pramono, E., Suharso, Rochliadi, A & Arcana, I. M. (2019). Cellulose nanofibers preparation from cassava peels via mechanical disruption. *Fibers, 7(44)*, 1-10. doi:10.3390/fib7050044

Yu, X., Tong, S., Ge, M., Wu, L., Zuo, J., Cao, C., & W. Song, (2013). Adsorption of heavy metal ions from aqueous solution by carboxylated cellulose nanocrystals. *Journal of Environmental Sciences, 25*(5), 933–943. doi:10.1016/j.fuel.2006.12.013.